Molecular mobility and Li^+ conduction in polyester copolymer ionomers based on poly(ethylene oxide)

Daniel Fragiadakis, Shichen Dou, Ralph H. Colby, and James Runt[a)]
Department of Materials Science and Engineering and Materials Research Institute, The Pennsylvania State University, University Park, Pennsylvania 16802, USA

(Received 20 August 2008; accepted 12 December 2008; published online 12 February 2009)

We investigate the segmental and local dynamics as well as the transport of Li^+ cations in a series of model poly(ethylene oxide)-based single-ion conductors with varying ion content, using dielectric relaxation spectroscopy. We observe a slowing down of segmental dynamics and an increase in glass transition temperature above a critical ion content, as well as the appearance of an additional relaxation process associated with rotation of ion pairs. Conductivity is strongly coupled to segmental relaxation. For a fixed segmental relaxation frequency, molar conductivity increases with increasing ion content. A physical model of electrode polarization is used to separate ionic conductivity into the contributions of mobile ion concentration and ion mobility, and a model for the conduction mechanism involving transient triple ions is proposed to rationalize the behavior of these quantities as a function of ion content and the measured dielectric constant. © *2009 American Institute of Physics*. [DOI: 10.1063/1.3063659]

I. INTRODUCTION

Polymer electrolytes play a critical role in energy storage and conversion devices such as batteries and fuel cells, enabling ion transport between the active components of the device. Despite the huge practical importance of these materials, and after several decades of research, many aspects of ion transport through polymers are incompletely understood, and progress in the field remains largely empirical. Poly(ethylene oxide) (PEO) was the first polymer found to have the ability to solvate various salts leading to complexes with significant conductivity, and is widely used, incorporated into various polymer architectures, in gel and solid-state polymer electrolytes.[1–5]

Both experimental studies and molecular dynamics simulations have provided valuable information on the basic mechanism of charge transport in polyether-based systems. It is generally agreed that conducting cations are complexed with several ether oxygen atoms (4–6 for PEO and Li^+ ions), strongly coupling cation mobility to polymer segmental mobility.[6,7] However, in polymer-salt electrolytes, conductivity is generally dominated by the motion of the anions (and/or triple ions) which is also enabled by segmental motion. From a practical point of view, it is desirable to maximize cation conductivity (transference number), while anion motion is undesirable as it decreases efficiency. Although segmental motion and conductivity have been directly measured and compared for a variety of polymer-salt electrolytes, very few such studies have been carried out on single-ion conductors, where conductivity is due solely to cation motion.

A crucial issue in polymer electrolytes is ion association.[8,9] Ions in polymer electrolytes are able to form pairs and larger aggregates, and conductivity is determined both by the number of mobile charges and their mobility. Although complexation with ether oxygens promotes dissociation of contact pairs, significant ion pairing is expected in the form of solvent-separated ion pairs or aggregates, given the low dielectric constant of PEO. The type and extent of ion association are not straightforward to obtain experimentally. Different definitions of "mobile" or "free" versus "immobile" or "bound" ions apply to different experimental techniques,[10] and in many cases it is not even clear that such a distinction can be made. Therefore, there is still disagreement on the main factor that limits conductivity: Is it a low degree of ion dissociation, due to the low dielectric constant, or low ion mobility due to strong interaction of the cations with the coordinating ether oxygen atoms?

This paper is part of our continuing investigation of ion transport in model polymer systems.[10–13] We study a series of PEO-based polyester copolymer ionomers. They are single-ion (Li^+) conductors, with sulfonate anions covalently bound to the polymer chains. The structure of the ionomers is shown in Fig. 1: the materials are similar to those studied in Ref. 11, where ion content was varied by changing the length of the PEO subchains. Here, instead, ion content is systematically varied by changing the ratio of ionic to nonionic isophthalate groups while keeping a fixed PEO segment molecular weight of 600 (13 EO repeat units). In this way, we are able to study a much wider range of ion contents, without the complications due to crystallization which occur for longer PEO segments.

The ionomers studied here have low conductivity for most practical applications (less than 10^{-5} S/cm at room temperature). However, these are excellent model systems for studying cation conduction in polymer electrolytes: they are single-phase materials, amorphous liquids at room temperature, with no ion clustering of the type typically observed in ionomers, and the conduction measured is due ex-

[a)]Electronic mail: runt@matse.psu.edu.

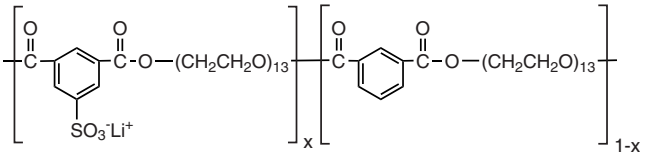

FIG. 1. Chemical structure of the polyester random copolymer ionomers PE600-*x*Li.

clusively to the motion of Li^+ ions. Also, ion content is varied systematically over a much wider concentration range than that of previous studies of single-ion conducting polymer electrolytes.[11,14–16]

II. EXPERIMENT

A. Sample preparation

The ionomers, as well as the corresponding neutral polymer, were synthesized by a two-step melt polycondensation process. Poly(ethylene glycol) (PE600, M_n=600 g/mol, 99%), triphenyl phosphate (TPP, 97%), titanium (IV) isopropoxide (99.999%), lithium chloride (99+%), and dimethyl isophthalate (DMI, 99%) were supplied by Aldrich. Dimethyl 5-sulfoisophthalate sodium salt (DM5SIS, 98%) was supplied by Alfa Aesar. All reagents were used without further purification.

The monomers were degassed in a vacuum oven for 12 h at 80 °C before use. A dry glass reactor (purged three times using argon) with a mechanical stirrer and three openings was charged with the appropriate amount of the oligomeric diol, diesters and catalyst titanium (IV) isopropoxide (0.05 wt %). The temperature of the reaction was maintained at 210 °C for 4 h and then 230 °C for 2 h. The byproduct methanol was removed using a liquid nitrogen cold trap. Diesters (12 mol % of diols) and triphenyl phosphate (0.05% of total reagents) were added after the mixture in the reactor was cooled to 180 °C and the reaction temperature was raised to 250 °C and maintained at this temperature for 2–3 h. The total molar ratio of diols to diesters was controlled at 1:1. Vacuum was applied for the final 0.5–1 h at 250 °C to remove low molecular weight species. The completion of the reaction was signaled by a rapid increase in viscosity, at which point the reactor was refilled with argon gas and cooled to room temperature.

The sodium polyester ionomers prepared above were dissolved in water and then diafiltered with de-ionized water using an Amicon 1000 molecular weight cutoff membrane. They were then dissolved in 0.5*M* $LiCl/H_2O$ and diafiltered to exchange the cations to Li^+. The concentrated ionomer solution was then freeze dried and then vacuum dried at 120 °C to constant mass.

Samples with various ion contents were synthesized by varying the ratio of sulfonated (DM5SIS) and neutral (DMI) isophthalates. They are labeled PE600-*x*Li where *x* is the fraction of ionic isophthalate groups. In the following, by "fraction of ionic groups" of an ionomer we are referring to the fraction of isophthalate groups that are sulfonated. ^{1}H NMR was used to confirm the structure of the polymer and determine the number-average molecular weights shown in Table I. Also shown in the table are the total ion content p_0 determined by ^{1}H NMR, the ratio of the number of ethylene oxide (EO) units to Li^+ ions, and a rough approximation of the average distance r_{av} between ionic groups, assuming that they are homogeneously distributed throughout the material.

TABLE I. Number average molecular weight, total ion concentration, ratio of ethylene oxide units to Li^+ ions and average distance between anions.

Sample	M_n (g/mol)	p_0 (cm^{-3})	EO/Li	r_{av} (nm)
PE600	12000	0	···	···
PE600-6%Li	4300	4.6×10^{19}	232	2.8
PE600-11%Li	6500	9.0×10^{19}	119	2.2
PE600-17%Li	11000	1.4×10^{20}	77	1.9
PE600-49%Li	6800	3.9×10^{20}	26	1.4
PE600-Li	4700	7.5×10^{20}	13	1.1

B. Experimental techniques

1. Thermal characterization

Glass transition temperatures (T_g) were determined using a TA Q100 differential scanning calorimeter. All experiments were performed under a dry nitrogen purge. Sample sizes were ~8 mg. All samples were heated to 363 K, held at that temperature for 5 min, then cooled to 183 K at 5 K/min. Samples were then heated to 363 K at 10 K/min, with T_g defined as the midpoint of the heat capacity change.

2. Dielectric relaxation spectroscopy

Samples for dielectric relaxation spectroscopy measurements were placed onto a brass electrode and dried in a vacuum oven at 353 K for 24 h, after which a second brass electrode was placed on top of the sample. Silica spacers were used to control the sample thickness at 50 μm. A Novocontrol GmbH Concept 40 broadband dielectric spectrometer was used to measure the dielectric permittivity. Frequency sweeps were performed isothermally from 10 MHz to 0.01 Hz in the temperature range from 143 to 393 K. In order to minimize the amount of water in the samples and to avoid a change in water content during the experiment, the samples were initially held at 393 K for 1 h, and the measurements were performed during subsequent cooling under a flow of dry N_2. Although the lower ion content samples slowly crystallize when stored below ~273 K, no crystallization occurred during the dielectric measurements (in similar samples, even for small amounts of crystallinity, a pronounced decrease in both the real and imaginary parts of the dielectric permittivity is observed on crystallization).

Dipolar relaxations were analyzed by fitting the dielectric loss ε'' or derivative spectra using the appropriate form of the Havriliak–Negami equation

$$\varepsilon^*_{HN}(f) = \frac{\Delta\varepsilon}{[1+(if/f_{HN})^a]^b} \quad (1)$$

for each relaxation process, where $\Delta\varepsilon$ is the relaxation

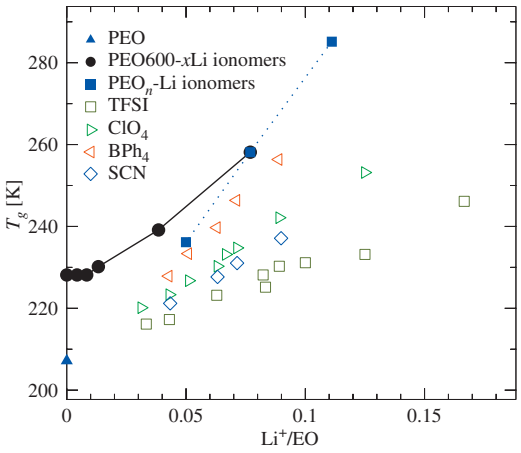

FIG. 2. (Color) Calorimetric glass transition temperatures of the polyester copolymer ionomers, polyester ionomers with variable PEO length (Ref. 11) (PE400-Li and PEO900-Li) and literature data for PEO-salt electrolytes containing BPh_4 (Ref. 46), SCN (Ref. 46), ClO_4 (Refs. 17 and 46), and TFSI (Refs. 17 and 46) anions. Ion concentration is expressed in Li^+ ions per EO unit. Uncertainties for measured T_gs are ±2 K.

strength, a and b are shape parameters and f_{HN} is a characteristic frequency related to the frequency f_{max} of maximum loss by

$$f_{max} = f_{HN}\left(\sin\frac{a\pi}{2+2b}\right)^{1/a}\left(\sin\frac{ab\pi}{2+2b}\right)^{-1/a}. \quad (2)$$

The analysis of conductivity and electrode polarization (EP) is described in Secs. III D and III E, respectively.

III. RESULTS AND DISCUSSION

A. Glass transition temperature

The nonionic polyester PE600 and all the ionomers show a single glass transition. The calorimetric T_g of the nonionic polymer is 228 K, significantly higher than that of neat PEO due to the presence of the rigid isophthalate groups in the chain structure. With increasing ion content, T_g remains constant for low ion content and then increases, reaching 258 K for 100% ionic isophthalate groups.

In Fig. 2 the glass transition temperatures are compared to literature values for PEO and various PEO-lithium salt electrolytes. Due to the extremely fast crystallization of PEO, it is very difficult to obtain reliable T_g measurements of PEO or of its mixtures with low salt content; a value of 206 K is shown for neat PEO.[17] The T_g increase in the copolymer ionomers is comparable to those of PEO containing a comparable amount (in terms of Li^+ ions per EO unit) of salts with low lattice energy, such as $LiClO_4$ or TFSI. Also included are glass transition temperatures for a previously studied series of PEO-based polyester ionomers,[11] identical in chemical structure to PE600-Li but with varying length of the PEO segment. In that series of ionomers, the T_g increase is much steeper than that of the copolymer ionomers since by decreasing PEO length one increases both the number of ions *and* the number of rigid isophthalate groups incorporated into the polymer chain, both acting to increase T_g.

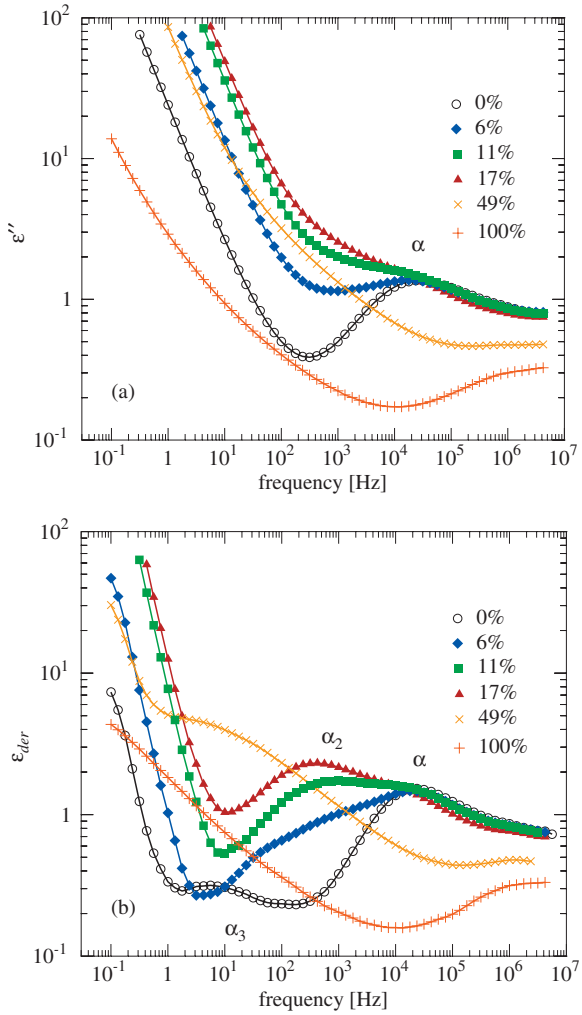

FIG. 3. (Color) (a) Dielectric loss and (b) derivative spectra at 253 K for the neutral copolymer and the ionomers.

B. Dielectric relaxation

Figure 3(a) shows typical dielectric loss spectra for the ionomers above T_g. Since the large values of dielectric loss at low frequencies due to conduction and EP mask any low-frequency loss peaks, we used the derivative formalism[18] to resolve dipolar processes in this temperature range

$$\varepsilon_{der}(f) = -\frac{\pi}{2}\frac{\partial\varepsilon'(f)}{\partial \ln f}.$$

(The derivative formalism is typically used, in the absence of EP and for relatively broad loss peaks, as a good approximation to "ohmic conduction-free" dielectric loss. In the presence of EP, the EP peak observed in the dielectric loss has a corresponding contribution to ε' therefore it is also present as a peak in the derivative spectrum. However, the width of the EP peak is considerably reduced in the $\varepsilon_{der}(f)$ spectrum compared to the corresponding peak in $\varepsilon''(f)$, allowing the dipolar processes present at higher frequencies to be resolved.)

In the derivative spectra of Fig. 3(b), we observe three relaxation processes: α, α_2, and α_3 in the order of decreasing frequency. The α process is observed for all samples, α_2 appears only in the ionomers and a weak, low-frequency α_3

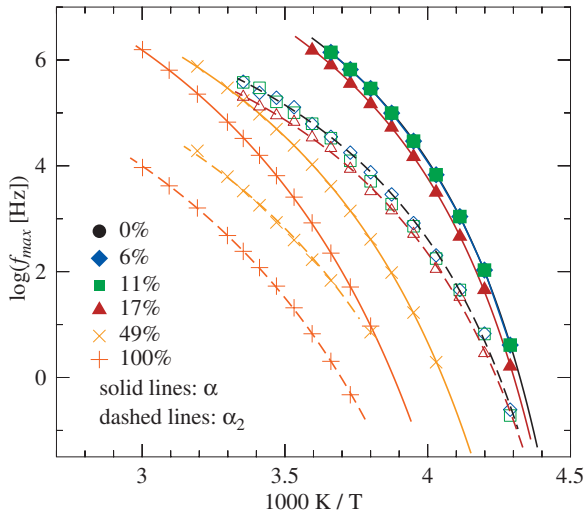

FIG. 4. (Color) Relaxation frequencies of the α and α_2 processes as a function of inverse temperature. Lines indicate fits of the VFT equation [Eq. (3)] to the data. Symbols for 0%, 6%, and 11% are on top of each other.

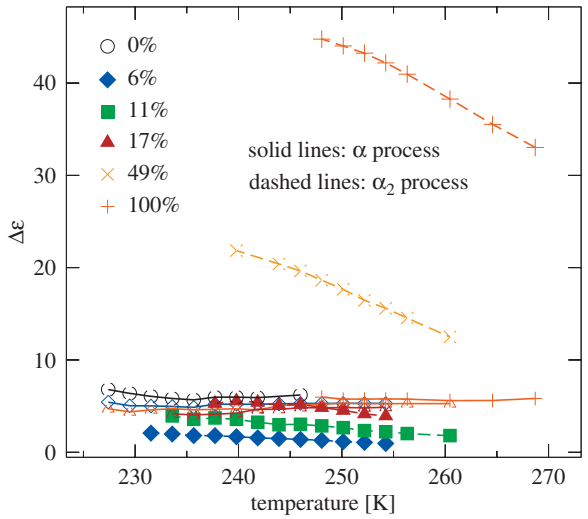

FIG. 5. (Color) Relaxation strengths of the α and α_2 processes as a function of temperature.

process is only possible to resolve for the neutral polymer, PE600-6%Li and PE600-11%Li. Arrhenius plots and corresponding fit parameters for the α and α_2 relaxations are displayed in Fig. 4 and Table II. Dielectric increments are plotted against temperature in Fig. 5.

1. α process (segmental mode)

The higher-frequency process, α, corresponds to the segmental relaxation of the polymer. The frequency position of the α process does not change for low ion content (up to 11% ionic groups), in agreement with the calorimetric T_g. At higher ion content, as T_g increases, the relaxation shifts to lower frequencies. The relaxation strength of the process does not change significantly with ion content and remains close to the value of $\Delta\varepsilon_\alpha \simeq 7$ of the neutral polymer.

The relaxation frequency of the α process is well described by the Vogel-Fulcher-Tammann (VFT) equation, as is usual for cooperative relaxations

$$f_{\max} = f_0 \exp\left(-\frac{DT_0}{T-T_0}\right), \tag{3}$$

where f_0 is a constant, T_0 the Vogel temperature, and D the so-called strength parameter. D quantifies the divergence from Arrhenius temperature dependence; higher D corresponds to less fragile, or more Arrhenius-like, behavior. Interestingly, the pre-exponential factor f_0 and Vogel temperature T_0 of the α process remain constant within experimental error, while above 10% ionic isophthalate groups the strength parameter D increases with increasing ion content, corresponding to a decrease of fragility. According to the usual interpretation for the increase of T_g with increasing ion content, complexed cations act as transient cross-links slowing down the relaxation of the polymer chains. The decrease in fragility is unexpected, since an increase in cross-linking density in a polymer network usually results in more fragile behavior.[19–21] A decrease in fragility with increasing ion content has been observed for the conductivity of other PEO-based electrolytes (although not directly for the segmental relaxation time), suggesting that it may be a more general phenomenon.[22,23] To explain this behavior, it was proposed that the ions increase T_g by acting as intrachain, rather than interchain, cross-links, increasing the rigidity of the polymer chains.[23] However, it is not clear why such an increase of chain rigidity would lead to less fragile behavior.

2. α_2 process (ion mode)

The α_2 process occurs in the ionomers at frequencies approximately two orders of magnitude lower than that of the α process. Its relaxation strength increases roughly proportionally to ion content and at high ion contents is much larger than that of the segmental process. The frequency of

TABLE II. Parameters of the VFT equation for the α, α_2, and α_3 processes and dc conductivity.

	α process			α_2 process			dc conductivity			α_3 process		
Sample	log f_0 (Hz)	D	T_0 (K)	log f_0 (Hz)	D	T_0 (K)	log σ_0 (S/cm)	D	T_0 (K)	log f_0 (Hz)	D	T_0 (K)
PE600	10.3	3.3	203									
PE600-6%Li	10.0	3.6	200	8.6	3.4	201	−4.6	3.3	201	8.0	4.5	193
PE600-11%Li	10.1	3.9	198	8.8	3.8	199	−3.9	3.6	199	9.2	5.8	185
PE600-17%Li	9.8	4.0	197	8.5	3.7	199	−3.5	3.9	198			
PE600-49%Li	10.0	5.3	200	8.5	5.6	200	−2.4	4.9	200			
PE600-Li	10.7	6.7	203	8.4	6.9	200	−2.0	5.7	203			

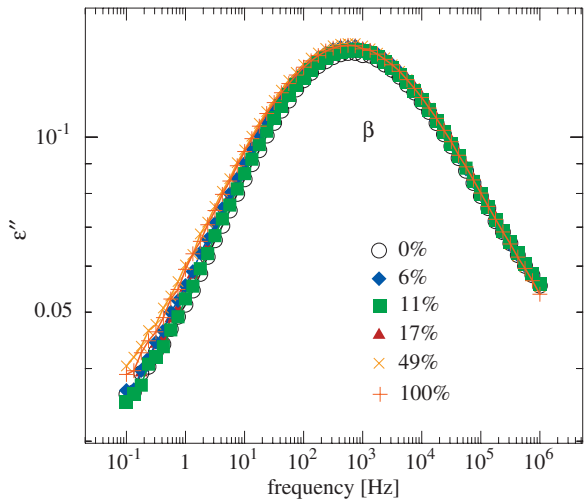

FIG. 6. (Color) Representative dielectric loss spectra in the temperature region of the β relaxation (173 K).

the α_2 process follows a VFT temperature dependence, and the Vogel temperature and strength parameter for α_2 closely follow those of the α process. Two possibilities appear for the interpretation of this process: a slowed-down segmental relaxation of PEO segments complexed with cations, or localized ion motion. The large dielectric increment $\Delta\varepsilon_{\alpha_2}$, which reaches 45–50 for PE600-Li (Fig. 5), leads us to conclude that ion motion must primarily be responsible for this process.

A so-called ion mode is observed for polyether-salt complexes, and is described as arising from fluctuation of ions in temporary confinement created by structural inhomogeneities.[24–26] We propose a more specific interpretation of this process, in terms of ion pairs: Given the low dielectric constant of PEO, Coulomb interactions between anions and cations will not be effectively screened and formation of ion pairs will be favored. These can be contact ion pairs or separated ion pairs, mostly the latter due to the ability of PEO to solvate the cations.[4,10,27] A natural interpretation of the ion mode, then, is that it arises from motion of cations in the vicinity of the anions, or in other words rotation of ion pairs. The large dielectric increment of the α_2 process is also reflected in a significant increase in the static dielectric constant with ion content, and the quantitative analysis of the static dielectric constant in Sec. III C strongly supports the assignment of the α_2 process to rotation of ion pairs. The frequency position of the relaxation is also consistent with this assignment: for ion motion over the scale of a few angstroms to occur, several rearrangements of the neighboring polymer segments must take place. The location of the relaxation, one to two orders of magnitude slower than the segmental process, but with identical Vogel temperature, is therefore reasonable.

Relaxation processes attributed to slowed-down segmental motion of complexed polymer segments have been observed for several polymer-salt complexes using dielectric spectroscopy[24] and quasielastic neutron scattering[28] as well as in molecular dynamics simulations.[29] Relaxation of complexed polymer segments is unlikely to appear at a frequency lower than that of the ion mode, since ion motion on the several angstrom scale must involve several rearrangements of complexed PEO segments. Such a relaxation, if it were to be observed separately, would have to be faster than the ion mode but slower than the segmental process of uncomplexed chains. It is more likely, however, that the cooperativity volume of the alpha process includes both complexed and uncomplexed segments. As a result, we believe that the slowing down of segmental motion due to complexation with cations is observed as a shift of the α process toward lower frequencies with increasing ion content, rather than the appearance of a second, slowed-down process. Note that PPO–$LiClO_4$ mixtures, where a hindered segmental process was observed at lower frequencies than the ion mode,[24] are phase separated into ion-rich and ion-poor microdomains and exhibit a double glass transition, unlike our polyester ionomers.[11]

3. α_3 process

For the neutral polyester as well as PE600-6%Li and PE600-11%Li, a weak third process appears at an even lower frequency than the α_2 process, also following a VFT temperature dependence. At higher ion contents this process, if present, cannot be resolved from the much stronger α_2 peak. Its dielectric strength is subject to large error due to the overlap with the α_2 process, however, it seems to remain approximately constant at $\Delta\varepsilon_{\alpha_3} \simeq 1-2$, independent of ion content.

The origin of the α_3 process is not yet clear. We do not expect to observe a normal-mode (terminal relaxation) process, since the molecule does not possess a dipole moment component parallel to the main chain. Some clues about the origin of this process may be provided by the structure of these polymers: small-angle and ultrasmall angle x-ray scattering profiles, which will be the subject of a future publication, exhibit a large amount of scattering at low wavevectors for all samples including the nonionic polyester. This suggests that even though the samples do not phase separate in the conventional sense, they may, in fact, show a nanoscale structure, perhaps resulting from incompatibility between the PEO and isophthalate segments [analogous to nanophase separation in poly(*n*-alkyl methacrylates)].[30] Even if this is the case, however, it is not clear that this would lead to an additional low-frequency dielectric relaxation.

4. β process

Both the neutral polymer and the ionomers exhibit a single broad β relaxation, associated with local chain twisting in the PEO segments[31] (Fig. 6). The relaxation frequency and dielectric strength of the process remain practically unchanged with ion content. This is despite the fact that, at least for PE600-49%Li and PE600-Li, a significant fraction of PEO segments is expected to be coordinated with Li ions: assuming that, on average, each Li ion is coordinated with five EO segments, nearly 40% of all EO segments will be coordinated in PEO600-Li. Therefore, we expected to observe a significant effect on the dielectric strength of the β process. In poly(2-vinyl pyridine)-$LiClO_4$ mixtures, for example, the local β relaxation of the pyridine group, which coordinates with Li ions, is strongly suppressed with increas-

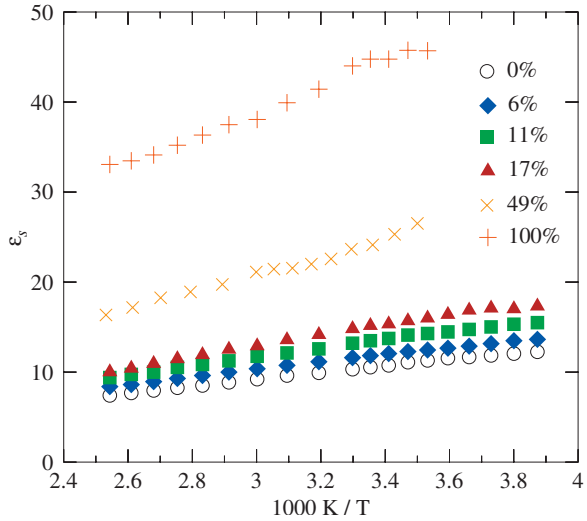

FIG. 7. (Color) Static dielectric constant vs inverse temperature.

ing salt content.[26] This is not the case in the polyester ionomers, where the only effect observed is a very slight broadening of the peak on the low-frequency side.

C. Static dielectric constant

The static dielectric constant ε_s, shown in Fig. 7, was obtained from the low-frequency plateau of the $\varepsilon'(f)$ spectra after subtracting the contribution of EP. The dielectric constant for the ionomers increases with increasing ion content, and reaches values of around 45 for PE600-Li. PEO-based polyester[12] and polyurethane[10] ionomers with related chemical structures show very similar behavior. The analysis of dipolar relaxations in Sec. III B allows us to identify the origin of the increase in ε_s: comparing Figs. 5 and 7, we see that the increase in dielectric constant is due exclusively to the increase in dielectric strength of the ion mode (α_2 process), i.e., to rotation of ion pairs.

The dielectric constant is related to the dipole moment of the relaxing units through the Onsager equation[32,33]

$$\frac{(\varepsilon_s-\varepsilon_\infty)(2\varepsilon_s+\varepsilon_\infty)}{\varepsilon_s(\varepsilon_\infty+2)^2}=\frac{\nu m^2}{9\varepsilon_0 kT}, \tag{4}$$

where ν and m are the number density and dipole moment of the dipoles, respectively, ε_∞ is the high-frequency limit of the dielectric constant, ε_0 is the permittivity of vacuum, and k is Boltzmann's constant.

The Onsager equation can be extended to take into account multiple types of dipoles, ν_i and m_i being the number density and dipole moment, respectively, of dipoles of type i:

$$\frac{(\varepsilon_s-\varepsilon_\infty)(2\varepsilon_s+\varepsilon_\infty)}{\varepsilon_s(\varepsilon_\infty+2)^2}=\frac{1}{9\varepsilon_0 kT}\sum_i \nu_i m_i^2. \tag{5}$$

Separating the contribution of the ion pairs from that of the polymer chains, we can write

$$\sum_i \nu_i m_i^2=\nu_{\text{pair}} m_{\text{pair}}^2+\left[\sum_i \nu_i m_i^2\right]_{\text{PE600}}.$$

Substituting into Eq. (5) and rearranging, we obtain the relation

$$\nu_{\text{pair}} m_{\text{pair}}^2=9\varepsilon_0 kT\left(\frac{(\varepsilon_s-\varepsilon_\infty)(2\varepsilon_s+\varepsilon_\infty)}{\varepsilon_s(\varepsilon_\infty+2)^2}-\left[\frac{(\varepsilon_s-\varepsilon_\infty)(2\varepsilon_s+\varepsilon_\infty)}{\varepsilon_s(\varepsilon_\infty+2)^2}\right]_{\text{PE600}}\right). \tag{6}$$

From Eq. (6) we can calculate the number density of ion pairs given the pair dipole moment, or vice versa. For the high-frequency limit of the dielectric constant we use an approximate value of $\varepsilon_\infty=n^2$, where $n=1.454$ is the refractive index of PEO. Making the approximation that all the ions form pairs ($\nu_{\text{pair}}=p_0$), we find a pair dipole moment of approximately $m_{\text{pair}}\simeq 10-12$ D, independent of temperature, for all samples. Since we ignore unpaired ions, as well as interactions between ion pairs which would probably reduce the effective pair dipole moment, m_{pair} should be treated as a lower limit for the dipole moment of an ion pair. Our values for m_{pair} are considerably larger than the dipole moment of $m_{\text{CP}}=5.5-7$ D for a sulfonate-Li contact ion pair (depending on the dielectric constant of the surrounding medium), obtained using *ab initio* quantum mechanical calculations which will be the subject of a future publication. It is difficult to estimate the value of m_{SP}, the dipole moment of a separated pair, since we expect a range of separated pair configurations corresponding to the various possibilities for cation complexation with the surrounding ether oxygen atoms.[34] However, values of m_{SP} in the range of 10–15 D are reasonable, corresponding to a larger average distance between ionic centers and therefore a larger dipole moment, than a contact pair. This strongly suggests that (a) a significant fraction of the ions are present in the form of separated ion pairs (taking a rough estimate of $m_{\text{CP}}\simeq 7$ D and $m_{\text{SP}}\simeq 15$ D, we obtain that ~60% of pairs are separated pairs) and (b) the degree of ion pairing is independent of temperature in the temperature range examined spanning ~150 K. Note also that the strong decrease in the dielectric constant with increasing temperature does not reflect a decrease in the number of ion pairs but is related to the factor $1/T$ that appears in Eq. (5), arising from thermal randomization in the Onsager model.

D. Conductivity

Figure 8 displays the dc conductivity, as determined by fitting the linear portion of the dielectric loss curves in the low-frequency region, using

$$\varepsilon''(f)=\frac{\sigma_{\text{dc}}}{2\pi f\varepsilon_0}. \tag{7}$$

With increasing ion concentration the high-temperature dc conductivity increases, and the curves shift toward higher temperatures due to the slowing down of polymer mobility. A realistic analysis must account for a possible change in the number of mobile carriers with temperature. However, the dependence of σ_{dc} on temperature can be fit very well by the VFT equation

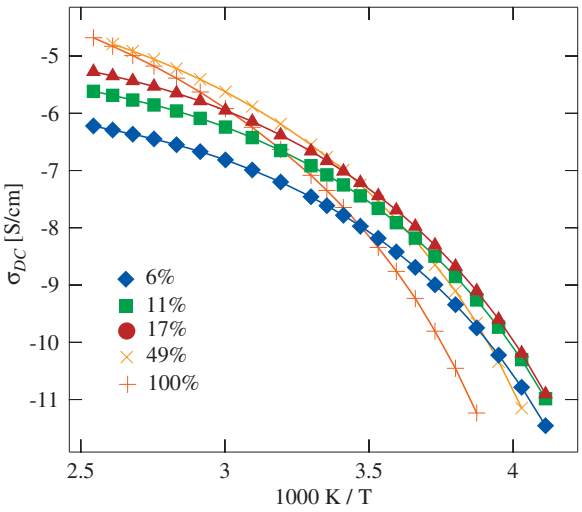

FIG. 8. (Color) dc conductivity as a function of inverse temperature for the copolymer ionomers. Lines are fits of Eq. (8), with parameters listed in Table II.

$$\sigma_{\mathrm{dc}} = \sigma_0 \exp\left(-\frac{DT_0}{T - T_0}\right). \tag{8}$$

The fit parameters σ_0, T_0, and D are given in Table II. The Vogel temperature T_0 is close to 200 K, independent of ion concentration, equal, within experimental error, to that of the α and α_2 relaxation times. The strength parameter D is close to that of the α and α_2 process, increasing with increasing ion content. This confirms that for all ion contents there is *strong coupling between macroscopic ion transport, ion pair rotation and segmental motion*.

In order to investigate the mechanism of conduction in more detail, we normalize the conductivity by the total number of ions via the molar conductivity $\Lambda = \sigma_{\mathrm{dc}}/p_0$. In the literature, conductivity is often normalized with respect to the glass transition temperature by plotting against $T - T_g$ or T/T_g, in order to account for the slowdown of segmental motions with the increase in ion content. Since the shape of the temperature dependence, quantified by the parameter D, also changes with ion content, we plot instead in Fig. 9 the molar conductivity against the segmental relaxation frequency f_α and ion mode frequency f_{α_2}.

For ion motion strongly coupled to polymer segmental motion, conductivity is expected to obey the Debye–Stokes–Einstein (DSE) equation. If the number of charge carriers is independent of temperature, this can be written as

$$\Lambda \propto f_\alpha. \tag{9}$$

Deviations from this behavior are observed very often, both for low-molecular weight liquids and for polymers. Conductivity is often described instead by a power law,[35–38]

$$\Lambda \propto f_\alpha^s, \tag{10}$$

with $s < 1$ (fractional DSE equation). For all of the copolymer ionomers, conductivity scales with the segmental relaxation frequency according to Eq. (10), with $s = 0.88 \pm 0.02$. Similar behavior is observed for Λ against the frequency of the ion mode relaxation α_2, with exponent $s = 0.88 \pm 0.04$. Two suggestions have been made to rationalize this type of

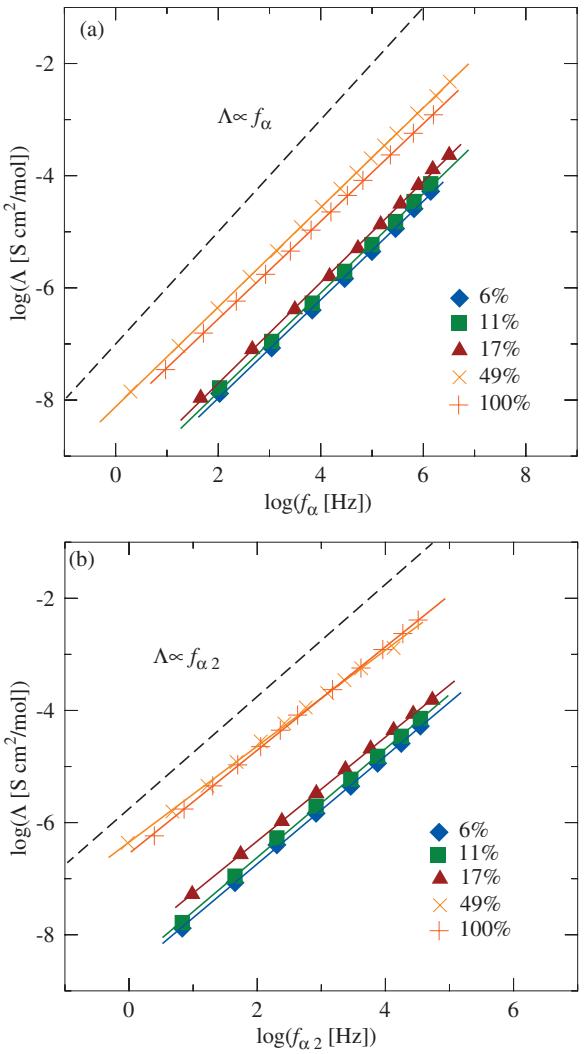

FIG. 9. (Color) Molar conductivity vs segmental (a) and ion mode (b) relaxation frequency. Solid lines are fits of Eq. (10) to the data, the dotted line indicates a slope of 1 [Eq. (9)].

behavior: (a) a decoupling of translational motion from segmental motion, which is an intrinsic characteristic of the dynamics of the material,[37,38] or (b) a change in the number of charge carriers with temperature.[39] Note that if we accept the latter interpretation, the number of mobile carriers would have to *decrease* with increasing temperature.

The curves in Fig. 9 separate into two groups: PE600-49%Li and PE600-Li have significantly higher conductivity, per ion, than the low ion content ionomers, at a fixed frequency of the segmental process. We cannot attribute this to decoupling of conductivity from segmental motion, since for all samples $\Lambda \propto f_\alpha^{0.88}$, indicating that the ion transport mechanism is coupled in the same way to polymer mobility. However, it is clear that a change in the conduction mechanism takes place at higher ion content. From the results of Fig. 9 it is not possible to distinguish whether the increase in molar conductivity is due to a larger fraction of ions contributing to conduction in the high ion content ionomers, or to an increase in ion mobility, and plausible arguments could be made to support either scenario. Our approach to separating ion concentration and mobility effects, based on the analysis of EP, is presented in the following section.

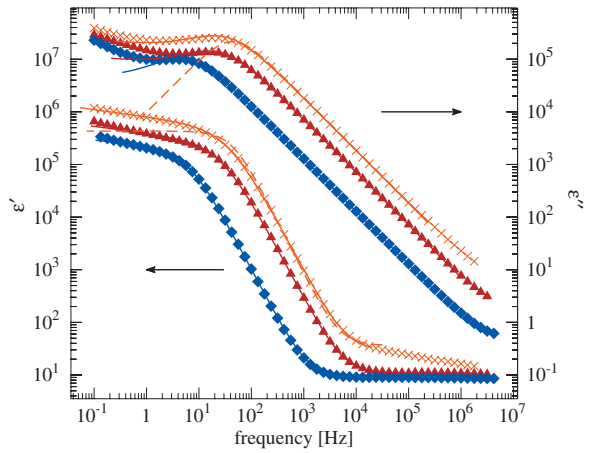

FIG. 10. (Color) Real part ε' and imaginary part ε'' of the dielectric permittivity at 363 K for the ionomers PE600-6%Li (◇), PE600-17%Li (△), and PE600-Li (x). Solid lines are fits of the modified Macdonald model [Eq. (13)]. For PE600-Li, the fits of the original Macdonald model [Eq. (12)] are shown for comparison as dashed lines.

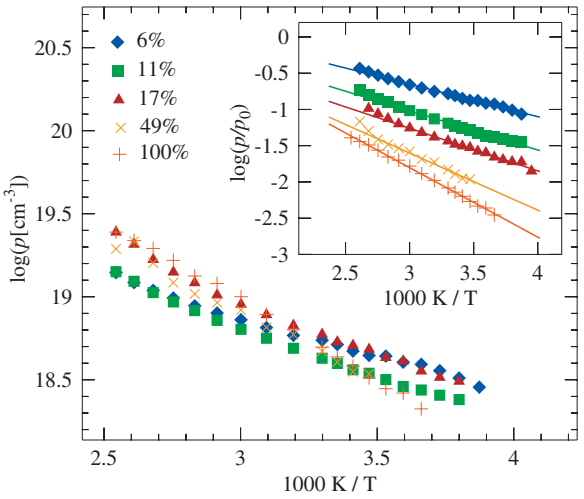

FIG. 11. (Color) Number density of mobile ions p from the EP model vs inverse temperature. The inset shows p divided by the total ion concentration. Lines are fits of Eq. (14) to the data, with parameters listed in Table III.

E. Analysis of electrode polarization

Conductivity can be expressed as the sum over all charge carriers of the product of ion concentration, ion mobility and ion charge

$$\sigma_{\mathrm{dc}} = \sum_{i=1}^{n} p_i \mu_i q_i, \tag{11}$$

where p_i, μ_i, and q_i are the concentration, mobility and charge of the ith type of charge carrier, respectively. In our case only one type of carrier, Li^+ ions, can be mobile, therefore $\sigma_{\mathrm{dc}}=p\mu q$, where q is the elementary charge.

Measurements of EP can be used to separate conductivity into the contributions of mobile ion concentration p and ion mobility μ.[12,40,41] EP is the accumulation of charge at the interfaces between an electrolyte and blocking electrodes, when applying a low-frequency ac electric field. EP is observed in dielectric spectroscopy measurements as large apparent values of dielectric constant and dielectric loss at low frequencies. Typical dielectric spectra in the region where EP dominates the response are shown in Fig. 10.

According to Macdonald's model of EP, in the case of a single mobile carrier, the contribution of EP to the complex dielectric function can be modeled as a macroscopic Debye relaxation[42,43]

$$\varepsilon^*_{\mathrm{EP}}(f) = \frac{\Delta\varepsilon_{\mathrm{EP}}}{1 + i2\pi f\tau_{\mathrm{EP}}}, \tag{12}$$

with an apparent relaxation time of

$$\tau_{\mathrm{EP}} = \frac{L}{2L_D}\frac{\varepsilon_0\varepsilon_s}{q\mu p}$$

and an apparent dielectric increment

$$\Delta\varepsilon_{\mathrm{EP}} = \left(\frac{L}{2L_D} - 1\right)\varepsilon_s,$$

where

$$L_D = \left(\frac{\varepsilon_0\varepsilon_s kT}{q^2 p}\right)^{1/2}$$

is the Debye length, L is the electrode spacing and ε_s is the static dielectric constant. In the presence of EP, Eq. (12) replaces the usual dc conductivity contribution of Eq. (7). Note that τ_{EP} and $\Delta\varepsilon_{\mathrm{EP}}$ depend differently on p and μ, allowing the separate determination of each from the dielectric data.

We analyze the dielectric spectra using an empirical modification of the Macdonald model[10]

$$\varepsilon^*_{\mathrm{EP}}(f) = \frac{\Delta\varepsilon_{\mathrm{EP}}}{(i2\pi f\tau_{\mathrm{EP}})^{1-n} + i2\pi f\tau_{\mathrm{EP}}} \tag{13}$$

retaining Macdonald's expressions for τ_{EP} and $\Delta\varepsilon_{\mathrm{EP}}$. Equation (13) is mathematically equivalent to a constant phase element-type equivalent circuit, widely used for modeling EP[44] and provides a much better fit to the experimental data at low frequencies than the original Macdonald model. The exponent n is $0<n\leq 1$ and has been connected with electrode roughness.[45]

Before discussing the results, we mention a few criticisms of this type of analysis. First of all, it is not clear that in systems where distances between ionic groups are of the order of a few nm at most, one can make a clear distinction between associated, immobile ions on one hand and mobile ions on the other. This distinction, implied even in Eq. (11), is a necessary simplification in order to proceed. As far as limitations of the particular model used this, model (1) ignores interaction between ions, and is thus restricted to very low ion concentrations; (2) ignores the image charges on the electrodes. Sawada[41] recently proposed a model incorporating the image charges, but this model also predicts a different dependence of τ_{EP} on sample thickness ($\tau_{\mathrm{EP}}\propto L^2$) than the one predicted by the Macdonald model and observed for our ionomers ($\tau_{\mathrm{EP}}\propto L$).[12] With these caveats in mind, we present the results of the EP analysis since they are reproducible, systematic with ion content and potentially very useful for obtaining a complete picture of ion transport.

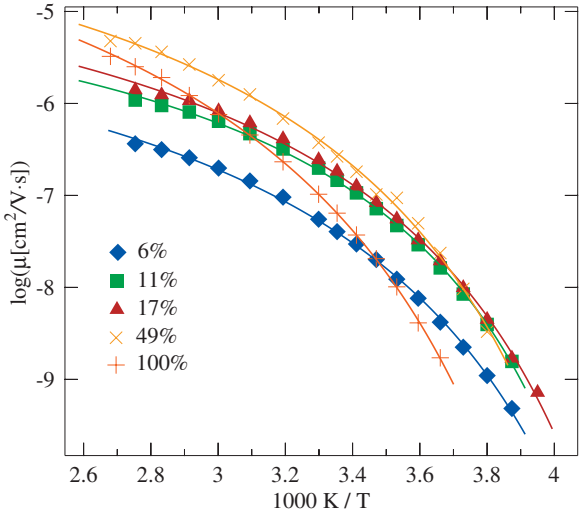

FIG. 12. (Color) Ion mobility, determined from the EP model, vs inverse temperature. Lines are fits of Eq. (16) to the data, with parameters listed in Table III.

1. Ion concentration

Figure 11 shows the fraction of mobile ions in the ionomers, determined using the EP model. The results are similar to those obtained using the same method for other single-ion conducting ionomers.[10,12] A small fraction of mobile ions is found, in agreement with the analysis of the static dielectric constant. The fraction of mobile ions increases with increasing temperature and the dependence of the mobile ion concentration is well described by an Arrhenius equation

$$p = p_\infty \exp(-E_a/kT), \tag{14}$$

where p_∞ is the mobile ion concentration as $T \to \infty$ and E_a is an activation energy. This temperature dependence can be explained in terms of thermal dissociation of solvent-separated ion pairs into unpaired ions.[10] In this case the activation energy E_a can be thought of as the binding energy of an ion pair.

The pre-exponential factor p_∞ is within an order of magnitude of, although systematically larger than, the total ion concentration p_0 determined from the stoichiometry. The activation energy of the 100% sulfonated ionomer is similar to that determined in our previous studies of fully sulfonated polyester and polyurethane ionomers with closely related chemical structures to the present samples. In the simplest case, E_a is given by the Coulomb energy

$$E_a = \frac{q^2}{4\pi\varepsilon_0\varepsilon_s r}. \tag{15}$$

Therefore, we would expect that the increase in the dielectric constant with increasing ion content would favor ion dissociation by lowering E_a. Instead an increase in E_a is observed, which leads to a decrease in the fraction of mobile ions with increasing total ion content (although the absolute number of mobile ions remains approximately constant). Even if we take ε_s to be the dielectric constant of the matrix immediately surrounding the ion pairs, which we approximate by the dielectric constant of the nonionic polymer, a constant value of E_a is predicted. According to Eq. (14), this would lead to an increase in the number of mobile ions with increasing total ion content. This suggests that this simple model is not sufficient to describe ion pairing in our ionomers, and additional effects resulting from ionic interactions, not taken into account by Eq. (15), play a significant role in determining the fraction of mobile ions at higher ion content.

2. Ion mobility

The ion mobility determined from the EP model is displayed in Fig. 12. The data are well described by a VFT equation

$$\mu = \mu_\infty \exp\left(-\frac{DT_0}{T - T_0}\right). \tag{16}$$

The VFT temperature dependence of ion mobility reflects the coupling of segmental motion and ion transport. Fitting parameters for the ion mobility are shown in Table III. To examine this correlation directly we plot ion mobility against the segmental relaxation frequency and ion mode relaxation frequency in Fig. 13 (the results for μ versus f_{α_2} are very similar). As is the case for the conductivity, ion mobility follows a fractional DSE type behavior

$$\mu \propto f_\alpha^n$$

with $n < 1$. The deviation from ideal DSE behavior is somewhat greater for the ion mobility than for the conductivity because the mobile ion content increases with temperature. This is also reflected in the VFT parameters of the mobility (Table III), where the Vogel temperature T_0 is 210–215 K for the mobility versus 200 K for both α and α_2 relaxation frequencies and conductivity.

In addition, at a fixed segmental relaxation frequency,

TABLE III. Fitting parameters for Eqs. (14) and (16) for the mobile ion concentration and ion mobility, respectively.

	Ion concentration		Ion mobility		
Sample	E_a (kJ/mol)	log p_∞ (cm^{-3})	log μ_∞ (cm^2/V s)	D	T_0 (K)
PE600-6%Li	8.4	20.3	−5.0	2.4	209
PE600-11%Li	10.0	20.5	−4.7	1.9	215
PE600-17%Li	10.8	20.8	−4.4	2.3	210
PE600-49%Li	15.6	21.3	−3.7	2.6	212
PE600-Li	18.2	21.7	−3.5	3.3	215

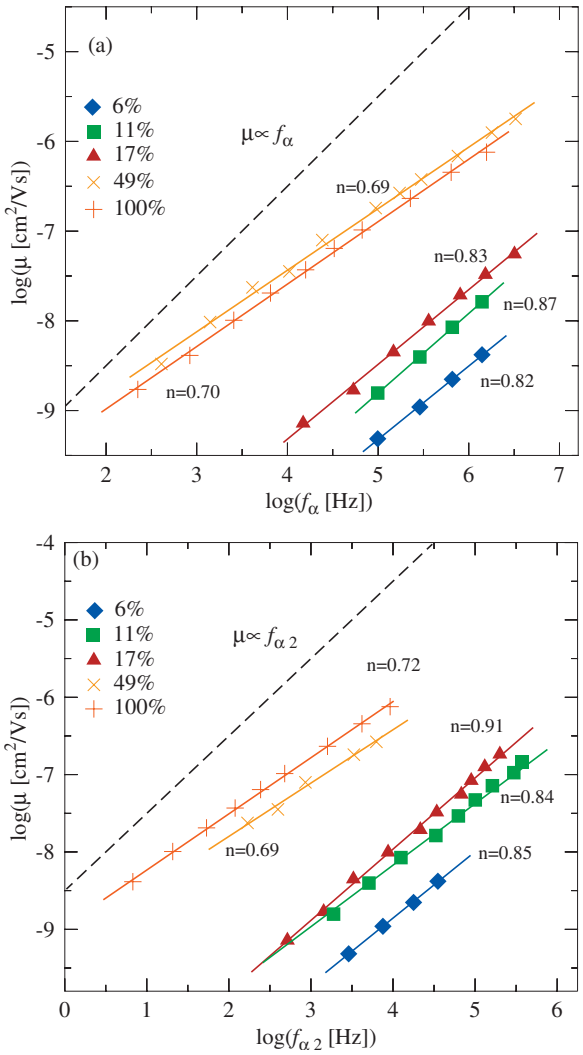

FIG. 13. (Color) Ion mobility against segmental (a) and ion mode (b) relaxation frequency. Lines are fits to $\mu \propto f^n$; best fit exponents n for each curve are given on the plots.

mobility *increases* by more than two orders of magnitude as we increase the fraction of ionic groups from 5% to 100%. As for the conductivity, the ionomers seem to separate into two groups, with PE600-49%Li and PE600-Li showing a significantly higher ion mobility than the low ion content ionomers, and in this case also a lower exponent n. To explain the increase in mobility, we propose a simple model for the conduction mechanism. Given the low mobile ion concentration, mobile ions move in an environment consisting mostly of ion pairs. Given the strong electrostatic interaction between ion pairs and mobile cations, it is reasonable to assume that the mobile ions interact with ion pairs forming transient $Li^+SO_3^-Li^+$ triple ions.[4] Since the sulfonate anions are attached to the polymer chains, we propose that ion motion must take place through a hopping mechanism of mobile cations transferring from one ion pair to a neighboring one. The mobility will therefore depend not only on segmental motion, but also on the potential barrier E_{hop} that the cation must overcome to move from one ion pair to the next. With increasing ion content, the distance between neighboring ion pairs decreases and their Coulomb potential wells increasingly overlap, decreasing E_{hop} and increasing mobility. The same mechanism, essentially, has been proposed by Bruce and Gray[4] to be active in polymer-salt electrolytes; a similar argument based on overlapping of Coulomb wells has been used to explain the increase in molar conductivity with ion content in PPO-salt systems.[35]

IV. SUMMARY

Molecular mobility and ion transport in a series of model PEO-based polyester copolymer ionomers with systematic variation of ion content were studied using dielectric relaxation spectroscopy. The ionomers are amorphous and exhibit a single glass transition temperature and no evidence of ion clustering.

Four dielectric relaxations were observed. The segmental α process slows down with increasing ion content above a critical concentration, showing decreasing fragility with increasing ion concentration. Two slower processes are present, the ion mode α_2, assigned to rotation of separated ion pairs, and a weak low-frequency α_3 process. The local β relaxation, due to local twisting of PEO segments, is apparently not significantly affected by complexation of ether oxygens with Li cations. In addition, analysis of the static dielectric constant using the Onsager equation suggests that the majority of the ions form separated ion pairs.

dc conductivity is strongly coupled with segmental motion over the entire range of ion content studied, and follows a fractional DSE relation. An increase in molar conductivity is observed for high ion content. Using a physical model of EP, dc conductivity was decomposed into the contributions of mobile ion concentration and ion mobility. The overall features of the ion concentration and mobility parallel those which have been observed for other single-ion conducting and polymer-salt polymer electrolytes, and are consistent with the general picture we have previously proposed.[10] This can be summarized as follows: Due to the low dielectric constant but strong Li-complexing ability of PEO, most ions are present as separated ion pairs. These thermally dissociate and release unpaired cations that rapidly form $Li^+SO_3^-Li^+$ triple ions. In addition, we propose a hopping mechanism for conductivity involving those transient triple ions, which rationalized the observed increase in ion mobility with increasing ion content. An independent investigation of mobile ion concentration and mobility, using complementary techniques, is underway and will be the subject of a future publication.

ACKNOWLEDGMENTS

The authors thank the Department of Energy, Office of Basic Energy Sciences, for support for this research through Grant No. DE-FG02-07ER46409. R.H.C. thanks Michael Rubinstein and Zhen-Gang Wang for helpful discussions.

[1] M. Armand, Solid State Ionics **69**, 309 (1994).
[2] P. V. Wright, MRS Bull. **27**, 597 (2002).
[3] D. F. Shriver and P. G. Bruce, Polymer Electrolytes I: General principles in *Solid State Electrochemistry*, edited by P. G. Bruce (Cambridge University Press, Cambridge, 1995).
[4] P. G. Bruce and F. M. Gray, in *Solid State Electrochemistry*, edited by P. G. Bruce (Cambridge University Press, Cambridge, 1995).
[5] M. Armand and J.-M. Tarascon, Nature (London) **451**, 652 (2008).

[6] M. Davies, P. J. Hains, and G. Willams, J. Chem. Soc., Faraday Trans. 2 **69**, 1785 (1973).
[7] J. J. Fontanella, J. J. Wilson, M. K. Smith, M. C. Wintersgill, C. S. Coughlin, P. Mazaud, S. G. Greenbaum, and R. L. Siddon, Solid State Ionics **50**, 259 (1992).
[8] Y. Marcus and G. Hefter, Chem. Rev. (Washington, D.C.) **106**, 4585 (2006).
[9] P. G. Bruce and C. A. Vincent, J. Chem. Soc., Faraday Trans. **89**, 3187 (1993).
[10] D. Fragiadakis, S. Dou, R. H. Colby, and J. Runt, Macromolecules **41**, 5723 (2008).
[11] S. Dou, S. Zhang, R. J. Klein, J. Runt, and R. H. Colby, Chem. Mater. **18**, 4288 (2006).
[12] R. J. Klein, S. Zhang, S. Dou, B. H. Jones, R. H. Colby, and J. Runt, J. Chem. Phys. **124**, 144903 (2006).
[13] R. J. Klein, D. T. Welna, A. L. Weikel, H. R. Allcock, and J. Runt, Macromolecules **40**, 3990 (2007).
[14] X.-G. Sun and C. A. Angell, Solid State Ionics **175**, 743 (2004).
[15] W. Xu, M. D. Williams, and C. A. Angell, Chem. Mater. **14**, 401 (2002).
[16] D. P. Siska and D. F. Shriver, Chem. Mater. **13**, 4698 (2001).
[17] C. Vachon, C. Labrèche, A. Vallée, S. Besner, M. Dumont, and J. Prud'homme, Macromolecules **28**, 5585 (1995).
[18] M. Wübbenhorst and J. van Turnhout, J. Non-Cryst. Solids **305**, 40 (2002).
[19] N. M. Alves, J. L. Gómez Ribelles, and J. F. Mano, Polymer **46**, 491 (2005).
[20] J. K. W. Glatz-Reichenbach, L. J. Sorriero, and J. J. Fitzgerald, Macromolecules **27**, 1338 (1994).
[21] C. M. Roland, Macromolecules **27**, 4242 (1994).
[22] J. M. Cruickshank, H. V. S. A. Hubbard, N. Boden, and I. M. Ward, Polymer **36**, 3779 (1995).
[23] H. V. S. A. Hubbard, J. P. Southall, J. M. Cruickshank, G. R. Davies, and I. M. Ward, Electrochim. Acta **43**, 1485 (1998).
[24] T. Furukawa, Y. Mukasa, T. Suzuki, and K. Kano, J. Polym. Sci., Part B: Polym. Phys. **40**, 613 (2002).
[25] S. H. Zhang and J. Runt, J. Phys. Chem. B **108**, 6295 (2004).
[26] P. Atorngitjawat and J. Runt, J. Phys. Chem. B **111**, 13483 (2007).
[27] R. Frech, S. York, H. Allcock, and C. Kellam, Macromolecules **37**, 8699 (2004).
[28] A. Triolo, V. Arrighi, R. Triolo, S. Passerini, M. Mastragostino, R. E. Lechner, R. Ferguson, O. Borodin, and G. D. Smith, Physica B **301**, 163 (2001).
[29] O. Borodin and G. D. Smith, Macromolecules **39**, 1620 (2006).
[30] M. Beiner, Macromol. Rapid Commun. **22**, 869 (2001).
[31] N. G. McCrum, B. E. Read, and G. Williams, *Anelastic and Dielectric Effects in Polymer Solids* (Dover, New York, 1967).
[32] L. Onsager, J. Am. Chem. Soc. **58**, 1486 (1936).
[33] *Broadband Dielectric Spectroscopy*, edited by F. Kremer and A. Schönhals (Springer-Verlag, New York, 2002).
[34] O. Borodin, G. D. Smith, O. Geiculescu, S. E. Creager, B. Hallac, and D. DesMarteau, J. Phys. Chem. B **110**, 24266 (2006).
[35] M. G. McLin and C. A. Angell, Solid State Ionics **53–56**, 1027 (1992).
[36] C. A. Angell, Annu. Rev. Phys. Chem. **43**, 693 (1992).
[37] S. Corezzi, E. Campani, P. A. Rolla, S. Capaccioli, and D. Fioretto, J. Chem. Phys. **111**, 9343 (1999).
[38] M. Paluch, T. Psurek, and C. M. Roland, J. Phys.: Condens. Matter **14**, 9489 (2002).
[39] M. G. McLin and C. A. Angell, J. Phys. Chem. **95**, 9464 (1991).
[40] H. J. Schütt and E. Gerdes, J. Non-Cryst. Solids **144**, 14 (1992).
[41] A. Sawada, J. Chem. Phys. **126**, 224515 (2007).
[42] J. R. Macdonald, Phys. Rev. **92**, 4 (1953).
[43] R. Coelho, J. Non-Cryst. Solids **131–133**, 1136 (1991).
[44] F. Bordi, C. Cametti, and R. H. Colby, J. Phys.: Condens. Matter **16**, R1423 (2004).
[45] T. Pajkossy, Solid State Ionics **176**, 1997 (2005).
[46] F. Lemaître-Auger and J. Prud'homme, Electrochim. Acta **46**, 1359 (2001).